

Confocal imaging of the exo- and endoskeleton of Protura after non-destructive DNA extraction

Alexander Böhm¹, Daniela Bartel¹, Nikolaus Urban Szucsich^{1,2} and Günther Pass^{1,3}

¹ Department of Evolutionary Biology, University of Vienna, Althanstraße 14, 1090 Vienna, Austria

² Biozentrum Grindel und Zoologisches Museum Hamburg, Universität Hamburg, Martin-Luther-King-Platz 3, 20146 Hamburg, Germany

³ Corresponding author: Günther Pass (e-mail: guenther.pass@univie.ac.at)

Abstract

In certain minute arthropods, such as Protura, species determination cannot be performed unambiguously without clearing and slide mounting of specimens. This causes an awkward dilemma for scientists conducting molecular research, since conventional DNA extraction entails destruction of the whole specimen. Thus, single individuals can be used either to obtain molecular data or for determination purposes. Such molecular datasets are thus dependent on determination of co-habitant specimens, and entries in GenBank are highly prone to misidentification.

To overcome this problem, we applied a non-destructive DNA extraction method and subsequently used confocal autofluorescence imaging to analyse and document cuticular characters of the same specimens. Alternatively the preparations can be examined by conventional microscopy. Our results show that the used non-destructive extraction method results in completely clear cuticular remains and does not significantly affect autofluorescence or shape. The acquired confocal image stacks and resulting volume renderings are useful to visualise, reconstruct and quantify structures for taxonomic purposes but also for morphological investigation of special cuticular structures such as the head endoskeleton of hexapods.

Keywords: Cuticle, CLSM, autofluorescence, Congo red

1. Introduction

Entries in DNA and RNA sequence databases lose much of their value if verification of species-identification is impossible due to missing vouchers (Pleijel et al. 2008). In minute soil arthropods, such as Protura, the problem is even more complex, since species can only be determined after clearing the specimens (Wilkey 1962). During the clearing procedure, however, the tissue, necessary to obtain sequence data, is destroyed completely. Species identification then is dependent on determination of co-habitant specimens (paragenophore of Pleijel et al. 2008). However, in a handful of soil a number of different species of Protura can exist. Christian & Szeptycki (2004), for example, found 23 different species of Protura at a single sampling site in a *Quercus pubescens* forest in Austria. Therefore, it is essential to preserve a determinable voucher by using a non-destructive DNA extraction method (NDE method). Presently, several such extraction methods are available (e.g. Porco et al. 2010 and references therein).

In the past decade, biological visualisation has become highly improved by methods of 3D data acquisition and reconstruction (for a review see Walter et al. 2010). In this context, several authors proposed to use the autofluorescence of arthropod cuticle in combination with CLSM imaging (e.g. Klaus et al. 2003, Klaus & Schawaroch 2006, Schawaroch & Li 2007). Subsequently, several conventional histological stains were shown to have fluorescent properties, leaving them useful for confocal microscopy of arthropod cuticle (Lee et al. 2009).

The most recently proposed dye for this purpose is Congo red (Michels & Büntzow 2010).

Aim of the present study is to evaluate whether non-destructive DNA extraction methods can be combined with confocal laser scanning microscopy (CLSM) for examination of cuticular characters of Protura. For this we tested the impact of NDE methods on the autofluorescent property of insect cuticle and compared the latter to Congo red stained specimens.

2. Material and Methods

2.1. Animals

Soil samples were collected on 26.IX.2009 at the Eichkogel [*Ionescuellum* sp., Austria, Lower Austria – N: 48° 03' 45,03'' E: 16° 17' 32,26'' (WGS84), 354 m.a.s.l.] under *Pinus nigra*, and 09.IX.2009 at the Leopoldsberg [*Acerentomon* sp., Austria, Vienna – N: 48° 16' 36,36'' E: 16° 21' 00,46'' (WGS84), 320 m.a.s.l.]. Animals were extracted using a Berlese-Tullgren funnel and stored in 100% EtOH. Determination was based on Nosek (1973). *Ionescuellum* sp. was identified as *I. carpaticum* (Ionesco, 1930) by Yun Bu, Shanghai Institutes for Biological Sciences, China. Species level determination was not attempted for *Acerentomon* sp. since this specimen was only used for Congo red staining of the head.

2.2. DNA Extraction

Two alternative NDE protocols were used which combine each a digestion buffer with two different extraction methods. Specimens are placed in a 2 ml tube, air dried, immersed in 180 µl digestion buffer (after Gilbert et al. 2007) and incubated for 2 hours at 55 °C with gentle agitation. The remaining cuticle is transferred into 70% EtOH and stored for further morphological analyses. DNA is purified from the digestion buffer using a phenol:phenol:chloroform extraction method and subsequent ethanol precipitation. The DNA pellet is resuspended in 50 µl ddH₂O. Alternatively, after digestion, a silica-based DNA purification method (DNeasy Blood & Tissue Kit, Qiagen) was used according to manufacturer's instructions, with a final elution step of 100 µl ddH₂O.

For the amplification of the fragments three different PCR conditions were used: (1) 10 cycles with 30 s at 95 °C, 30 s at 48 °C, and 30 s at 72 °C followed by 15 cycles with 60 s at 95 °C, 60 s at 56 °C, and 60 s at 72 °C; (2) 10 cycles with 60 s at 95 °C, 60 s at 52 °C, and 60 s at 72 °C followed by 40 cycles with 30 s at 95 °C, 30 s at 48 °C, and 30 s at 72 °C; (3) 30 cycles with 60 s at 95 °C, 60 s at 48 °C, and 60 s at 72 °C. A pre-denaturation of 5 min at 95 °C and a final extension step for 10 min at 72 °C were conducted.

Each PCR reaction consisted of 14 µl ddH₂O, 2 µl template (or ddH₂O as negative control), 2 µl primer [10 µM], 2.5 µl dNTPs [2.5 mM each], 2.5 µl PCR Buffer [2.5 mM], and 1 µl Polymerase [5 u/µl]. PCR products were either purified using QIAquick PCR Purification kit (Qiagen) or E.Z.N.A. ®Gel Extraction Kit (PeQLab), and eluted in 40 µl ddH₂O. For the sequencing reaction BigDye Terminator v3.1 Cycle Sequencing Kit (Applied Biosystems) was used. Cycle sequencing reactions were performed in 10 µl solutions (1 µl DNA, 1 µl Primer, 1 µl BigDye mixed with 7 µl ddH₂O). Conditions for the sequence reaction were

an initial denaturation step at 96 °C for 5 min, followed by 25 cycles of 20 s at 96 °C, 10 s at 50 °C and 4 min at 60 °C. The products of purification were sequenced on a capillary sequencer ABI PRISM 310x1 Genetic Analyzer at the Department of Evolutionary Biology, University of Vienna. Resulting electropherograms were visualised in ChromasLITE 2.01 (<http://www.technelysium.com.au>). Sequences from the forward and reverse strand were assembled manually in BioEdit Sequence Alignment Editor (Hall 1999) and were blasted against GenBank using the blastn option.

The first part (1400 bp) of the 28S rRNA (covering the Divergent Domains D1, D2 and D3) was amplified and sequenced in 2 overlapping fragments employing primers as specified in Dell'Ampio et al. (2009). To test our protocol we compared the DNA yield with specimens extracted destructively (DNeasy tissue kit, Qiagen).

2.3. Microscopy

After DNA extraction or conventional clearing with warm KOH the unstained cuticle was slide-mounted in polyvinyl-lactophenol (Waldeck GmbH, Münster, Germany). Cover slip spacers were made from adhesive tape or broken cover slips. Some specimens were stained for 1.5 days in an aqueous solution of 2 mg/ml Congo red at room temperature, dehydrated and embedded in Euparal (Waldeck GmbH, Münster, Germany).

Whole mounts were examined with a Leica TCS SP 2 confocal laser scanning microscope. Autofluorescence of the cuticle was excited with the 488 nm line of a Krypton-Argon laser. Table 1 contains information about the used objectives and image resolution. The proturan habitus (Fig. 2A) was stitched from three individual stacks using a Fiji (<http://pacific.mpi-cbg.de>) plugin by Preibisch et al. (2009). Volume renderings were generated with OsiriX (<http://www.osirix-viewer.org>). For z-projections we used Fiji's z-projection feature with the standard deviation or maximum intensity option. For some volume renderings of internal structures (Fig. 5A, B, C and Fig. 2D) the external cuticle was manually masked away in Fiji.

The image series for the excitation spectra (Fig. 1) were taken with a Leica TCS SP 5 X using a white light laser with emission adjustable from 470 nm to 670 nm (used step size 5 nm). The left side of the photomultiplier detection window moved with the increasing laser wavelength (10 nm offset) while the right side was fixed at 710 nm. The same instrument settings were used for both series.

Tab. 1 Information on the used objectives, number of z-slices and image resolution. Square brackets denote figures produced from the same dataset.

Figure	Objective	Number of z slices	Image resolution (pixel)
[2 A, A']	HC PL Fluotar 20.x, 0.5, dry	66	1024x1024
[2 B, C, D], [4 A, B, D / 5]	HXC PL Apo 40x, 1.25, oil	110, 270	1024x1024
[3]	PL Apo 100x, 1.40, oil	317	2048x2048
[1 B], [1 C], [4 C]	HXC PL Apo CS 63.0x, 1.30, glycerol	1, 1, 319	512x512, 1024x1024

3. Results & Discussion

3.1. DNA extraction and amplification

In total we extracted 21 individuals. In four instances the whole mount from the cuticular remains did not fulfil the requirements for determination due to awkward foldings which occurred during preparation.

18 individuals were amplified and 9 of these were sequenced. In all cases but one we received sequences and only one extraction did not work in PCR (despite average DNA yield). The DNA yield per individual ranged between 3 and 261 $\mu\text{l/ml}$ with an average of 144 ($n = 21$). Compared to specimens extracted conventionally by our working group (Dell'Amico et al. 2009), this average yield surprisingly is somewhat higher. The BLAST results gave us in all instances a proturan as best hit. Therefore contamination, e.g. from gut content, can be excluded. At least for highly repetitive genes, such as rRNA genes, our non-destructive DNA extraction works as well as the conventional DNA extraction methods. The non-destructive DNA extraction usually completely clears the cuticle of the specimens and leaves all characters important for determination, by conventional means or aided by CLSM imaging, intact.

In rare instances a small amount of tissue, which can be easily removed by a short KOH treatment, remains inside the cuticle. After DNA extraction, specimens can be treated like normal KOH cleared ones, since autofluorescence of the cuticle is not affected by the extraction procedure. Autofluorescence of proturan cuticle optimally is excited at 475 nm. By staining with Congo red the excitation peak of our sample moves to 555 nm (Fig. 1).

In the following two sections we will exemplarily demonstrate the usefulness of our approach for both taxonomic analysis and morphological investigation.

3.2. Visualisation of taxonomic characters: the tarsus of the proturan foreleg

The pattern of foretarsal sensilla is one of the most important diagnostic character complexes in proturan taxonomy. Determination by non-experts is highly complicated since it is difficult to assess the exact three-dimensional position of single sensilla and bristles when observed by a widefield microscope. Our volume renderings of CLSM datasets allow intuitive manipulation of the tarsus orientation and offer good resolution (Fig. 3). One drawback is the weaker signal from the backside of the tarsus that makes some sensilla appear rather faint (clearly recognizable but sometimes too faint for accurate length measurements). These different signal intensities can also lead to artificial thickness differences in volume renderings. Additionally, length measurements along the z axis in confocal image stacks cannot be made accurately without correcting for the inherent aberrations of the imaging technique. Good results are obtained by applying so called non-blind deconvolution algorithms that use a measured point spread function which is obtained by taking a confocal image stack of fluorescent beads (e.g. Difato et al. 2004). Decreasing signal in deeper layers of the sample is a common problem when acquiring CLSM stacks (Figs 2B, C and 3A). Leica CLSM software provides an intensity compensation function, however, we experienced difficulties in setting it up properly (e.g. visible in Fig. 2C, where the dorsal layers are brighter than more ventral ones, and the goal of homogeneous exposure over the whole stack depth is not met). Embedding samples between two coverslips and scanning from both sides is an obvious workaround for this problem (e.g. Klaus & Schawaroch 2006). To mitigate the problem of fluorescence attenuation with increasing penetration depth of the laser beam by image processing see suggestions provided by Sun et al. (2004).

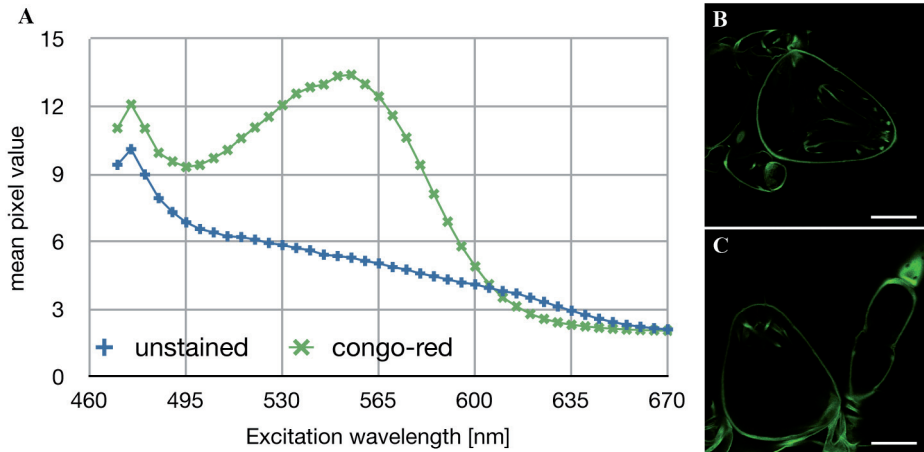


Fig. 1 **A:** Excitation spectrum of an unstained proturan head (+) and one stained with Congo red (x). Stained and unstained samples show an intensity peak at 475 nm but the Congo red stained sample has an additional broad peak at 555 nm. The mean pixel value of the respective whole image reflects the overall intensity of fluorescence. **B:** Head used for autofluorescence series (*Ionescuellum carpaticum*, 475 nm excitation) **C:** Congo red stained head (*Acerentomon* sp., 555 nm excitation). Scale bars: 50 μ m.

Congo red failed to stain the tarsal sensilla of Protura sufficiently. Its application resulted in a 25% gain in mean pixel value over an unstained specimen, given that both are excited with their respective optimal wavelength (Fig. 1). It must be noted that the vertical offset between both excitation spectra is partially due to the use of two different specimens and different embedding media. Regarding Protura, the contribution of Congo red to the total fluorescence is not the same for all cuticular structures, as is the case for at least some crustaceans (Michels & Büntzow 2010). Autofluorescence of unsclerotised cuticle, such as intersegmental membranes, is very low. Such regions stained with Congo red fluoresce almost as strongly as sclerotised regions (Fig. 4B versus C). Since sclerites are predominantly the focus of interest, staining with Congo red is mainly recommended for studies that investigate weakly sclerotised parts. The small intensity loss of unstained specimens can be easily compensated by adjusting the CLSM settings. It must be mentioned that Congo red staining fades within days in the acidic embedding medium polyvinyl-lactophenol, changing its colour to blue due to the pH indicator properties of this dye. Other embedding media, however, may avoid this problem and have better long term preservation properties (Klaus et al. 2003, Schawaroch & Li 2007). Michels (2007) found that Euparal embedding medium elicits a higher background than glycerol gelatine. For wavelengths smaller than 520 nm we likewise found a higher background for Euparal as compared to polyvinyl-lactophenol (up to +40% at 480 nm excitation). Essentially any mountant can be used as long as it is not strongly autofluorescent itself and its refractive index matches the immersion medium. This also implies that most existing preparations can be easily subjected to CLSM imaging.

3.3. Advanced analysis of cuticular structures: integument and head endoskeleton

Figure 2 A illustrates the usefulness of stack stitching to produce a high resolution dataset. Such stitching of a sufficient number of tiles allows for resolutions that plainly show all details necessary for determination. An image stack of the habitus then can be stored in a database

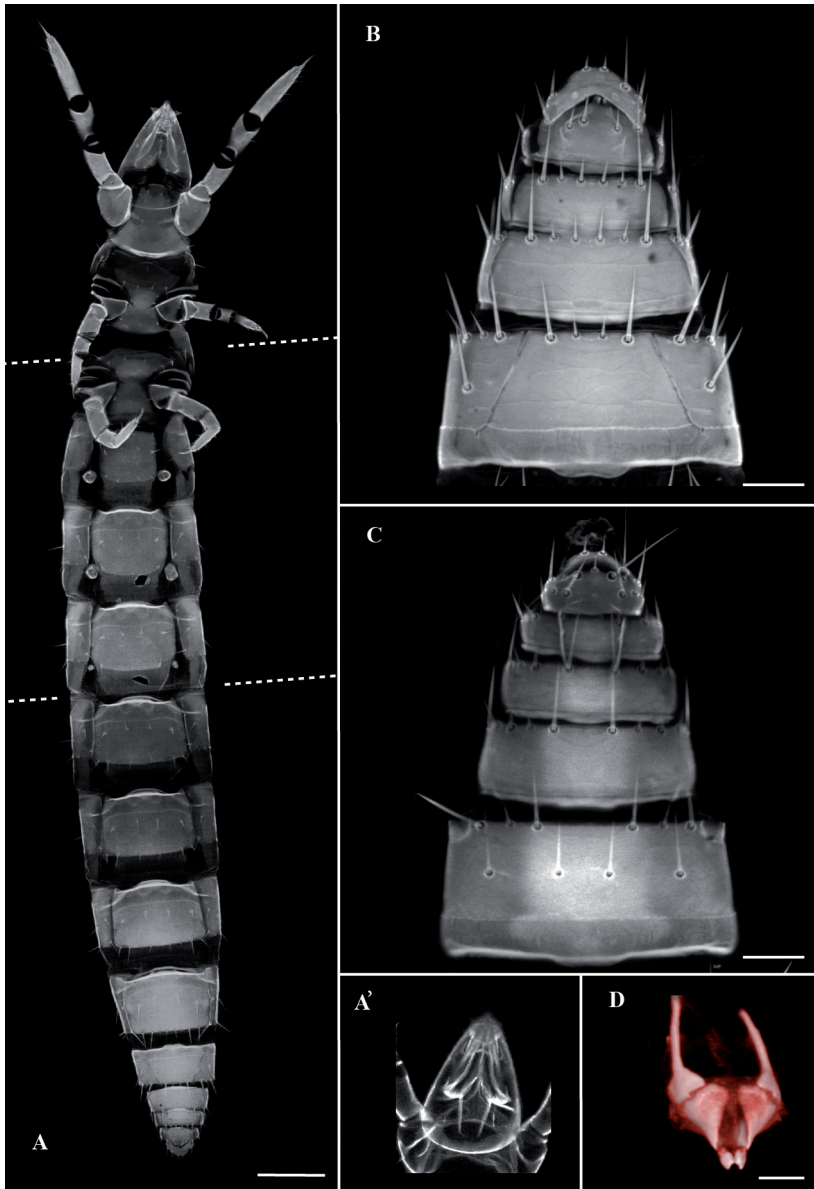


Fig. 2 *Ionescuellum carpaticum* Images A, B, C are standard deviation projections. **A**: Whole body fused from three individual stacks seen from ventral. Dashed lines show the stack borders. The two small holes at the hind margin of abdominal segments 2 and 3 were made with a needle after DNA extraction to reduce the risk of shrivelling of the cuticle during embedding (in later preparations this step was found to be superfluous). **A'**: Crop from the same stack but at a different depth. **B**: Ventral view of the abdominal tip. Superior exposure than in C because the specimen's ventral side faces upwards. **C**: Dorsal view of the abdominal tip. **D**: Volume rendering of the female genitalia prepared from the same dataset as B and C (view from above and behind). Scale bars: 100 μm (A), 25 μm (B, C), 10 μm (D).

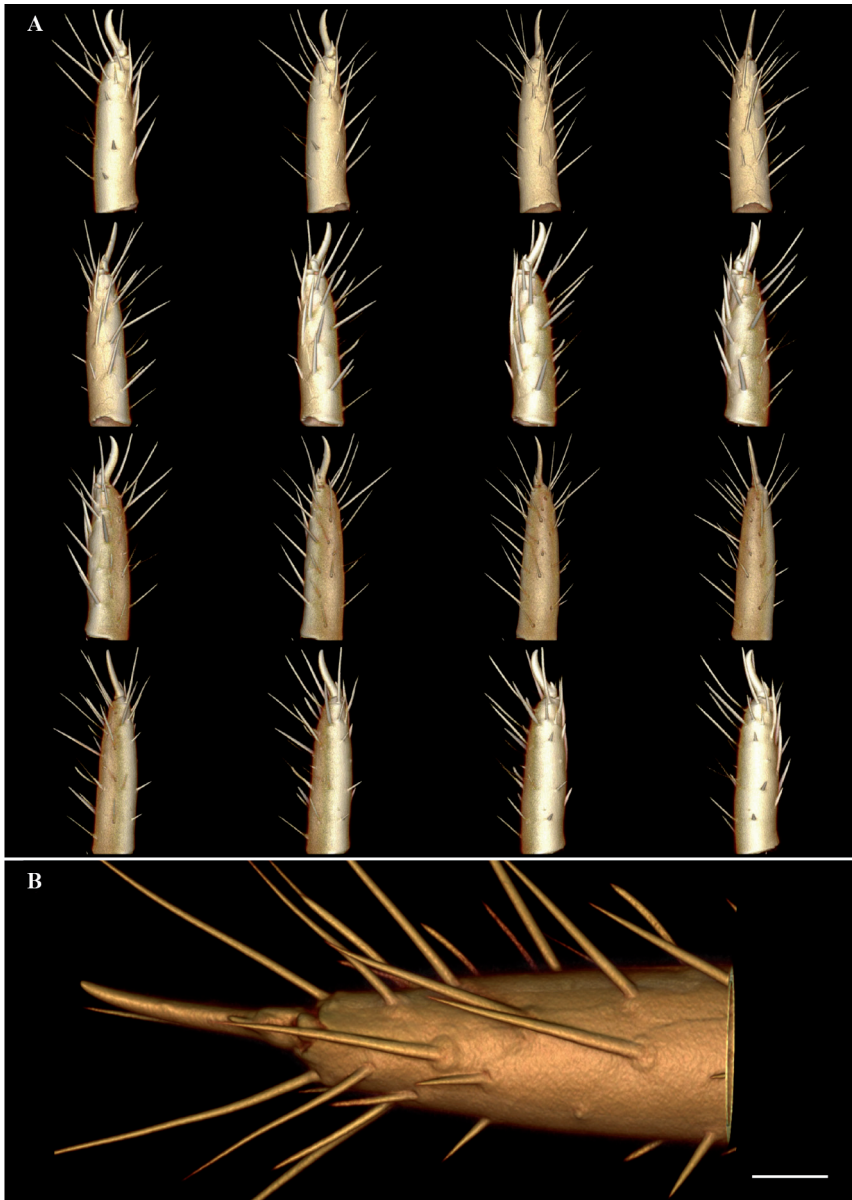


Fig. 3 Foretarsus of *Ionescuellum carpaticum*. **A:** 16 different views of the tarsus. Note that the ventral side is facing upwards on the slide and therefore this half of the tarsus shows brighter fluorescence. The bristles and sensilla on this ventral half are depressed by the cover slip. **B:** Detail of the foretarsus dataset (5x5 smoothing filter applied in OsiriX). Scale bar: 10 μ m.

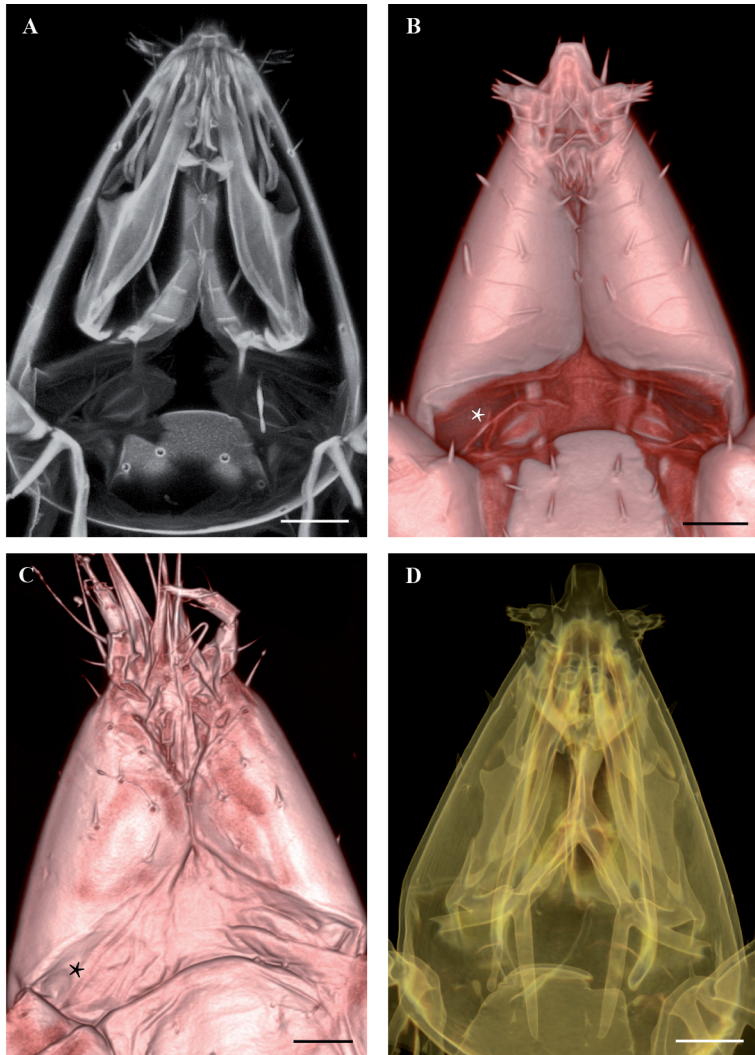


Fig. 4 Maximum intensity projection (A) and volume renderings of a head of *Ionescuellum carpaticum* (B, D) and *Acerentomon* sp. (C). C: Congo red stained. Note the strong fluorescence of the intersegmental membrane (*) as compared to B. The wrinkles of the membrane are caused by harsh dehydration. D: Different volume rendering settings help to reveal the internal head structures. Scale bars: 20 μm .

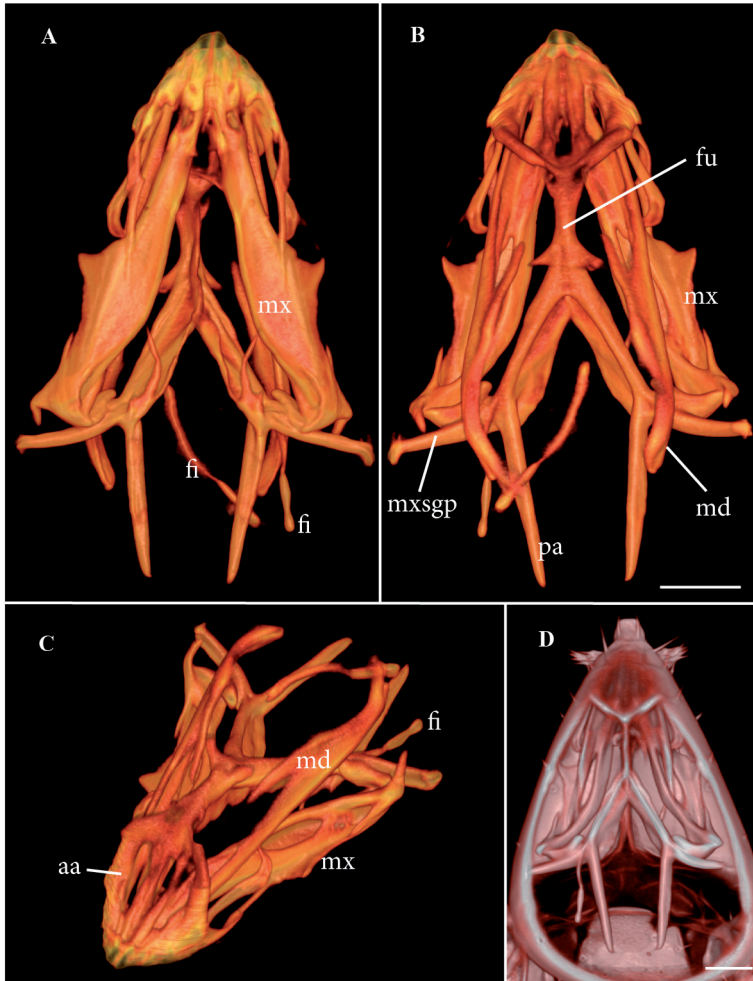


Fig. 5 Internal head structures of *Ionescuellum carpaticum* before (**D**) and after masking of the external cuticle (**A**, **B**, **C**). md = mandible, mx = maxilla, fu = fulcro-tentorium, aa = anterior arm of fu, pa = posterior arm of fu, mxsgp = maxillary sclerite of gnathal pouch, fi = filamento di sostegno. Nomenclature after François et al. (1992). Scale bars: 20 μ m.

together with the DNA sequences as a taxonomic voucher. With motorized microscope stages and advanced software the task of making stacks with many tiles will become even more convenient.

The head of Protura is an ideal object to show different visualisation techniques for internal and external structures (Fig. 4). Visualisation of internal structures by volume rendering is slightly more complicated than with z-projections. Normal cropping of the dataset (Fig. 5 D) is not entirely satisfying because some internal structures are either cropped or hidden by remaining external cuticle. One solution is to manually segment the structures of interest and make a surface reconstruction. This approach however is time-consuming and may not always be necessary. For figures 5A, B, C and 2D we segmented away the external cuticle, which can be done comparatively fast because only where internal structures are close to the external cuticle the latter has to be traced carefully. It should be kept in mind that a volume rendering normally cannot display all the information available in the original dataset, especially very high or low intensities. The right filamento di sostegno in Fig. 5B, for example, seems to be free-floating but in the sections the connection to its proximal duct is clearly visible.

For Protura, the methods employed by us provide the opportunity to combine unambiguous determination, which is only possible after clearing, with DNA extraction of the same specimen. CLSM autofluorescence imaging of proturan cuticle thus is a versatile tool for special tasks such as 3D visualisation and/or reconstruction of the foretarsus and other endo- and exoskeletal structures. Remaining shortcomings, like inexact assessment of sensillar dimensions can be easily overcome by light-microscopic analyses of the same whole mounts.

4. Supplementary Material

Supplementary material as well as a full colour version of this article is available at <http://www.soil-organisms.org>.

5. Acknowledgements

We like to thank Yun Bu for species determination, John Plant for improving the English and the core facility CIUS of the University of Vienna for providing access to the confocal microscopes. The appreciated comments of two anonymous reviewers helped to improve our manuscript

6. References

- Christian, E. & A. Szeptycki (2004): Distribution of Protura along an urban gradient in Vienna. – *Pedobiologia* **48**: 445–452.
- Dell’Ampio, E., N. U. Szucsich, A. Carapelli, F. Frati, G. Steiner, A. Steinacher & G. Pass (2009): Testing for misleading effects in the phylogenetic reconstruction of ancient lineages of hexapods: influence of character dependence and character choice in analyses of 28S rRNA sequences. – *Zoologica Scripta* **38**(2): 155–170.
- Difato, F., F. Mazzone, S. Scaglione, M. Fato, F. Beltrame, L. Kubínová, J. Janáček, P. Ramoino, G. Vicidomini & A. Diaspro (2004): Improvement in volume estimation from confocal sections after image deconvolution. – *Microscopy Research and Technique* **64**: 151–155.
- François, J., R. Dallai & W. Y. Yin (1992): Cephalic anatomy of *Sinentomon erythranum* Yin (Protura: Sinentomidae). – *International Journal of Insect Morphology and Embryology* **21**(3): 199–213.
- Gilbert, M. T. P., W. Moore, L. Melchior & M. Worobey (2007): DNA extraction from dry museum beetles without conferring external morphological damage. – *PLoS ONE* **2**(3): e272.

- Hall, T. A. (1999): Bioedit: a user-friendly biological sequence alignment editor and analysis program for windows 95/98/nt. – *Nucleic Acids Symposium Series* **41**: 95–98.
- Klaus, A. V., V. L. Kulasekera & V. Schawaroch (2003): Three-dimensional visualization of insect morphology using confocal laser scanning microscopy. – *Journal of Microscopy* **212**: 107–121.
- Klaus, A. V. & V. Schawaroch (2006): Novel methodology utilizing confocal laser scanning microscopy for systematic analysis in arthropods (Insecta). – *Integrative and Comparative Biology* **46**(2): 207–214.
- Lee, S., R. L. Brown & W. Monroe (2009): Use of confocal laser scanning microscopy in systematics of insects with a comparison of fluorescence from different stains. – *Systematic Entomology* **34**: 10–14.
- Michels, J. (2007): Confocal laser scanning microscopy: using cuticular autofluorescence for high resolution morphological imaging in small crustaceans. – *Journal of Microscopy* **227**(1): 1–7.
- Michels, J. & M. Büntzow (2010): Assessment of Congo red as a fluorescence marker for the exoskeleton of small crustaceans and the cuticle of polychaetes. – *Journal of Microscopy* **238**(2): 95–101.
- Nosek, J. (1973): The European Protura. Their taxonomy, ecology and distribution with keys for determination. – *Muséum d'Histoire Naturelle, Genève*, 346 pp.
- Pleijel, F., U. Jondelius, E. Norlinder, A. Nygren, B. Oxelman, C. Schander, P. Sundberg & M. Tholleson (2008): Phylogenies without roots? A plea for the use of vouchers in molecular phylogenetic studies. – *Molecular Phylogenetics and Evolution* **48**(1): 369 – 371.
- Porco, D., R. Rougerie, L. Deharveng & P. Hebert (2010): Coupling non-destructive DNA extraction and voucher retrieval for small soft-bodied Arthropods in a high-throughput context: the example of Collembola. – *Molecular Ecology Resources* **10**: 942–945.
- Preibisch, S., S. Saalfeld & P. Tomancak (2009): Globally optimal stitching of tiled 3D microscopic image acquisitions. – *Bioinformatics* **25**(11): 1463–1465.
- Schawaroch, V. & S. C. Li (2007): Testing mounting media to eliminate background noise in confocal microscope 3-D images of insect genitalia. – *Scanning* **29**(4): 117–184.
- Sun, Y., B. Rajwa & J. P. Robinson (2004): Adaptive image-processing technique and effective visualization of confocal microscopy images. – *Microscopy Research and Technique* **64**: 156–163.
- Walter, T., D. W. Shattuck, R. Baldock, M. E. Bastin, A. E. Carpenter, S. Duce, J. Ellenberg, A. Fraser, N. Hamilton, S. Pieper, M. A. Ragan, J. E. Schneider, P. Tomancak & J. Hériché (2010): Visualization of image data from cells to organisms. – *Nature Methods* **7**(3, Suppl.): S26–S41.
- Wilkey, R. F. (1962): A simplified technique for clearing, staining and permanently mounting small arthropods. – *Annals of the Entomological Society of America* **55**(5): 606.

Accepted 19 August 2011